Chemical Engineering Journal 207–208 (2012) 803–813

Contents lists available at SciVerse ScienceDirect

Chemical Engineering Journal

journal homepage: www.elsevier.com/locate/cej

Catalyst screening for conversion of glycerol to light olefins

Z.Y. Zakaria [a], J. Linnekoski [b], N.A.S. Amin [a,*]

[a] Chemical Reaction Engineering Group, Faculty of Chemical Engineering, Universiti Teknologi Malaysia, 81310 UTM Skudai, Malaysia
[b] VTT, Process Chemistry, Biologinkuja 7, B.O.Box 1000, FI-02044 VTT, Finland

HIGHLIGHTS

- Modified ZSM-5 catalysts were screened for conversion of glycerol to light olefins.
- Catalyst characterizations include XRD, FTIR, BET, TPD and TPR.
- Cu/ZSM-5 produced the highest light olefins selectivity and yield.
- Turnover frequency for Cu/ZSM-5 and Cr/ZSM-5 were high comparatively.

ARTICLE INFO

Article history:
Available online 25 July 2012

Keywords:
Glycerol to olefin
Catalytic conversion
Zeolite
Cracking
Dehydrogenation

ABSTRACT

Screening of modified ZSM-5 catalysts for conversion of glycerol to light olefins has been investigated. In this study HZSM-5, Al/ZSM-5, Ca/ZSM-5, Cr/ZSM-5, Cu/ZSM-5, Li/ZSM-5, Mg/ZSM-5 and Ni/ZSM-5 zeolite catalysts were prepared, tested and screened. The catalysts were characterized to relate their properties with catalyst activity. XRD and FTIR characterization results demonstrated that the structure of the catalysts remained intact while BET revealed the surface and micropore areas decreased after metal loading. TPR data exhibited the reduction phenomenon of the catalysts. NH_3-TPD analysis indicated that Cu/ZSM-5 catalyst has relatively more moderate and strong active acid sites compared to others. GC TCD/FID analysis detected light olefins and paraffins; methane, CO and CO_2 in the gaseous product stream. The acidity of the catalyst affected olefin production, but no direct correlation between surface area and olefin yield was observed. The turnover frequency (TOF) for Cu/ZSM-5 and Cr/ZSM-5 catalysts were significantly high comparatively. Cu/ZSM-5 produced the highest light olefins selectivity and yield due to the synergistic effect of the physico-chemical properties between the parent ZSM-5 and the metals.

1. Introduction

Biodiesel is an alternative fuel produced from renewable resources such as palm, canola, soya bean and rape seed oil [1]. It can be produced via transesterification reaction of fatty acids and alcohols. Approximately 10 wt.% of glycerol, an alcohol with three hydroxyl groups is produced as a byproduct in this reaction [2–4]. The crude glycerol obtained is about 50% pure and has a huge potential as raw material to produce other valuable products [5] in manufacturing of drugs, cosmetics, synthetic resins, ester gums and also in gas production [6]. With more crude glycerol being generated from biodiesel production as by-product, efforts to seek for economical ways to convert glycerol to useful chemicals continue which can indirectly minimize the cost of biodiesel production.

Glycerol can be converted to various precious products such as fuel additives [7], acrolein [5,8–10], propane [11] 1-hydroxyacetone [12], formaldehyde [5], acetol [5], alkyl aromatics [13], hydrogen [14] and many others. In several studies and reports involving glycerol dehydration [8,11,15,16] , light olefins have been detected as side product of the reaction. This finding was interesting since light olefins have such high commercial value and industrial importance. Up to date, no literature dedicated to investigating glycerol to light olefins has been reported. However, studies involving methanol and ethanol to light olefins over zeolite catalysts [17–20] are many inferring that glycerol, being in the same alcohol group as methanol and ethanol has the potential to be converted to light olefins.

Olefin is basically a petrochemical derivative conventionally produced by thermal cracking of natural gas and crude oil. Ethylene is the simplest olefin with only two carbon atoms. Major olefin products like ethylene, propylene, butadiene and C_4 derivatives, better known as light olefins are used to produce plastics, chemical intermediates, and industrial solvents [21]. The present cost of light olefin is very high and in the upward trend [22]. By utilizing glycerol and establishing a commercially viable process, there is huge potential to reduce the existing price of light olefins. In

* Corresponding author. Tel.: +60 7 5535553; fax: +60 7 55881463.
E-mail address: noraishah@cheme.utm.my (N.A.S. Amin).

1385-8947/$ - see front matter © 2012 Elsevier B.V. All rights reserved.
http://dx.doi.org/10.1016/j.cej.2012.07.072

addition, the overall process is environmentally friendly since the feed stock to produce light olefin is from renewable source.

The main objective of this study is to screen and investigate the catalytic performance of glycerol conversion to olefins. In order to achieve the objective, a set of ZSM-5 zeolite based catalysts were impregnated with metals across the periodic table. The structure of the modified catalysts was observed and characterized to provide better information about the relationship between the physico-chemical properties with catalyst activity. Different types of metals, namely lithium, magnesium, calcium, chromium, copper, nickel and aluminum were used to enhance the active acid sites on the zeolite catalyst surface and other physical properties. Catalyst characterizations employed were X-ray diffraction (XRD), Fourier Transform-Infra Red (FTIR), nitrogen adsorption (NA), temperature programmed desorption (TPD) and temperature program reduction (TPR). Products from the reaction were analyzed using GC TCD/FID from which the most promising catalyst was identified. The synergistic effect between the ZSM-5 zeolite and the metal loaded for the gas phase dehydration of glycerol was investigated.

2. Materials and methods

2.1. Materials

The main reagents used were HZSM-5 (SiO_2/nAl_2O_3 = 30; Zeolyst, USA in solid powder form), and liquid glycerol (87.5% purity; Merck, USA). The parent HZSM-5 catalyst was used as reference. Other chemicals were aluminum oxide purchased from Aldrich, calcium nitrate purchased from GCE Laboratory Chemicals, chromium nitrate from R&M Chemicals, copper nitrate from Emory Laboratory Reagents, lithium nitrate from Merck, magnesium oxide from GCE and nickel chloride from BDH Limited. We have used metal salts except for aluminum oxide and magnesium oxide which were in solid metal oxide form.

2.2. Catalyst preparation

Each metal-loaded ZSM-5 catalyst was prepared according to the wet-impregnation method. Initially, the parent HZSM-5 zeolite was added into 100 ml of distilled water. All metal nitrates, metal chloride and metal oxides, in their solid state, was then added into the solution, mixed and stirred at temperature 60–70 °C for an hour to make up a composition of 30% metal in each ZSM-5 catalyst. The solution was then dried at 100 °C for 12 h and finally calcined at 550 °C for 5 h. The calcined catalyst was then crushed and sieved between 40 and 50 mesh for a uniform catalyst size for the reaction with glycerol vapor.

2.3. Catalyst characterization

X-ray diffraction (XRD) was performed using Siemens Diffractometer D5000 (Software Diffract Plus) with CuKα radiation, λ = 1.54056 Å at 40 kV and 30 mA in the range of 2θ = 5°–50° at a screening speed of 0.05°/s, with a vertical ganiometer at room temperature (20 °C). The sample was held on a mountain sample holder and then grounded before being mounted on glass. Before analysis, the samples were saturated over concentrated NH_4Cl solution in a desiccator to ensure complete dehydration prior to pattern recording as this can affect the lattice parameter.

Infrared measurements were performed on a Perkin Elmer Spectrum One FT-IR spectrometer, with a spectral resolution of 2 cm^{-1}, scan time of 10 s using the KBr pellet technique. Thin wafers of 13 mm diameter were made by pressing about 10 mg of fine samples under 5 ton pressures for 15 s. The thin wafer was placed in a ring type sample holder and transferred into IR cell equipped with CaF_2 window and reading was carried out in vacuum system (1×10^{-8} mbar pressure) at room temperature.

The adsorption isotherm measurement was carried out by Quantachrome Autosorb-1, using nitrogen as the adsorbate at 77 K and the Micromeritics Accelerated Surface Area and Porosimetry (ASAP) 2000 equipment. The analyzer was calibrated using Al_2O_3 as the standard material prior to analysis. A known amount of sample was placed in the cell and out-gassed at 300 °C under vacuum for three hours. The adsorption isotherm was recorded point by point and the nitrogen volume, adsorbed at pressure p versus p/p_o was plotted.

The acidity of the catalyst was determined by temperature-programmed desorption of ammonia (NH_3-TPD) in a fixed-bed continuous flow micro-reactor at atmospheric pressure employing a thermal conductive detector (TCD). The samples (0.1 g) were dried at 200 °C for 1 h, and then ammonia-saturated in a NH_3 stream at 60 °C for 0.5 h. After purging with helium (30 ml/min) at 60 °C for 0.5 h to remove the physically adsorbed NH_3, the samples were heated at a linear heating rate of 20 °C/min up to 650 °C. In order to determine the acidity from the NH_3 desorption profiles, the areas under the curves were integrated by Gaussian deconvolution of the peaks and the acidity was expressed as micromoles of ammonia per gram of catalyst.

Temperature programmed reduction (TPR) was carried out in a quartz U-tube reactor with 20 mg of sample used for each measurement. Prior to reduction, the sample was pretreated in a He flow of 50 ml/min at 200 °C for 1 h and then cooled to room temperature. Subsequently, a H_2–Ar mixture (5% H_2 by volume) was introduced to the sample at a flow rate of 50 ml/min and the temperature was gradually increased from ambient to 650 °C at a rate of 20 °C/min. The hydrogen consumption was continuously monitored by a thermal conductivity detector (TCD) and was subsequently used to estimate the reduction degree of the catalyst by comparing with pure HZSM-5 as reference.

2.4. Catalyst evaluation

Catalyst testing was performed in a fixed-bed quartz reactor, with dimensions outside diameter = 13 mm and length = 35 cm, positioned inside a Carbolite tubular furnace. Prior to testing, the catalyst was activated in a flow of helium gas for 1 h at 500 °C. After the catalyst has been reduced, glycerol solution with 30% concentration was injected using a syringe pump into the system at flowrate = 0.1667 ml min^{-1} and vaporized between 300 and 310 °C before entering the reactor. Helium gas was used as carrier gas flowing at constant rate = 10 ml min^{-1}. A set of thermocouples attached to a temperature data logger was fixed along the line before the reactor to monitor the temperature at various locations. The purpose was mainly to ensure that glycerol would not condense before entering the reactor. The reaction was conducted at temperature = 600 °C, atmospheric pressure and WHSV = 105 Hr^{-1}. The catalytic testing was stopped after 25 min from the initial liquid glycerol injection. Gaseous products were collected in a gas sampling bag at every 5 min interval and further analyzed with a gas chromatograph equipped with both thermal conductive detector (TCD) and flame ionization detector (FID). The HP 6890 N GC–TCD/FID was equipped with HP plot/Q, HP-Mole sieve, GP-Gaspro and Hayasep-Q columns for main product analysis. The final amount as well as mass of liquid was recorded for the overall mass balance calculation which provided the amount of coke. The liquid was analyzed to trace unreacted glycerol for glycerol conversion calculation. Detail liquid analysis was not performed in this study since the focus was on light olefins production.

The conversion of glycerol, selectivity and yield of products are each defined by the following equations:

$$\text{Glycerol Conversion} = \frac{\text{Mol of glycerol converted}}{\text{Mol of glycerol in feed}} \times 100 \quad (1)$$

$$\text{Product Selectivity} = \frac{\text{Mass \% of product } i}{\text{Mass \% of feed}} \times 100 \quad (2)$$

$$\text{Product Yield} = \frac{\text{Mass \% of product } i}{\text{Mass \% of feed}} \times 100 \quad (3)$$

Only selectivity and yield to gaseous products, specifically light olefins, was discussed in this study in view of their commercial importance.

3. Results and discussion

3.1. XRD analysis

Fig. 1 illustrates the XRD patterns for all the prepared catalyst samples. The XRD patterns were analyzed between 5° and 50° with 2θ scale. The XRD pattern of the modified HZSM-5 completely matched with that of the parent HZSM-5, which indicates that the modification has no obvious effect on the parent zeolite structure [23]. There was also no new phase formation during heat treatment and zeolite modification. The XRD pattern of the modified zeolite indicates that the structure of the zeolites remains intact after loading different metals over the HZSM-5 catalyst. No peaks related to the metals were found from the diffractograms [24].

These patterns reveal that the metals were highly dispersed on the HZSM-5 catalyst for each of the metal-loaded catalyst. This finding is corroborated by the suggestions made by Jiang et al. [25], where no diffraction peaks corresponding to the metals were observed up to 40% loading. However, the intensities differed depending upon metal content. The highest intensity was observed for Cr/ZSM-5, followed by Al/ZSM-5, Ca/ZSM-5, Ni/ZSM-5, Cu/HZSM-5, Li/ZSM-5, and Mg/ZSM-5. The different intensities in the various samples may be due to higher absorption coefficient of the metals.

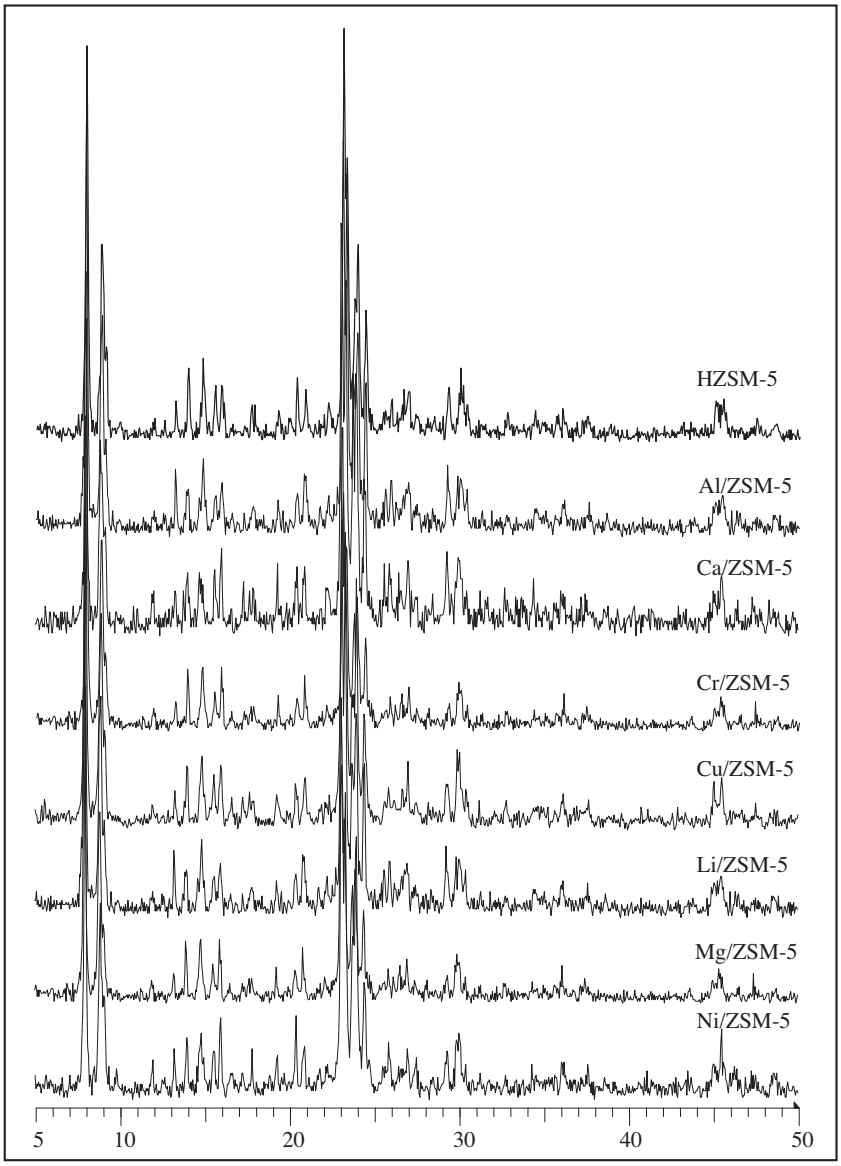

Fig. 1. XRD spectra for various impregnated metal ZSM-5 catalysts.

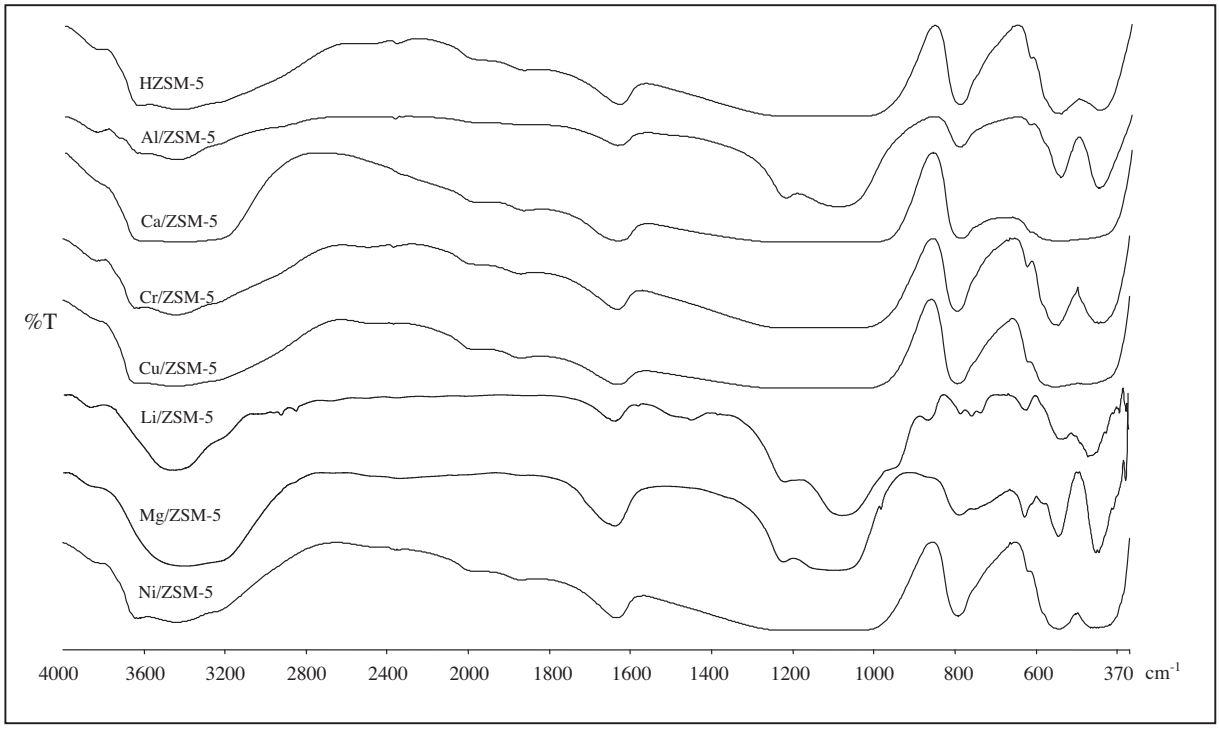

Fig. 2. Fourier Transform Infra-Red (FTIR) for various impregnated metal ZSM-5 catalysts.

3.2. FTIR analysis

The mid infra-red study range between 4000 cm^{-1} and 400 cm^{-1} that focused on the framework vibrations of zeolite was performed. From Fig. 2, it can be observed that there was no significant band position shifts, hence no isomorphous substitution in zeolite framework took place. This supports the prior discussion on XRD that the zeolite framework had remained intact. The water-bending vibration at 1640 cm^{-1} can be observed for all catalysts. It indicates the presence of adsorbed water in samples that occurred during incipient wet impregnation process. Another set of peaks can be observed at 1230 cm^{-1}, 1100 cm^{-1}, 796 cm^{-1} which are associated with asymmetric stretching vibrations of the Si–O–Si. These bands are related to internal linkages in SiO_4 or AlO_4 of zeolite lattices [25]. Unfortunately it was not possible to detect the impregnated metal inside the catalyst since the V_{T-O-T} value for bare metal ions namely Ni(II) and Mg(II) at 930 cm^{-1} and 937 cm^{-1} [26], respectively, could not be clearly detected within the individual spectra. This might be due to the fact similar to XRD where the presence of metals is not sufficient to be detected.

All catalyst samples generally exhibit O–H group in the 3600–3620 cm^{-1} band. The range is mainly attributed to the framework bridged hydroxyl groups (AlOHSi). This surface OH groups in zeolites basically originate from several sources of acidic spot such as: (1) OH groups due to framework Al, (2) silanol groups on the external surface and in the "nests" (defect sites), (3) OH groups attached to di- or tri-valent cation due to hydrolysis, (4) OH groups from "dangling Al", (5) OH groups associated with non-framework Al, and (6) OH groups of adsorbed water. The broad peak 3720–3740 cm^{-1} is associated with terminal silanol groups (SiOHs). Bands at ~3565, ~3630, ~3700 cm^{-1} which were less intense are ascribed to the H-bonded internal Si–OH, Si–OH nest, Si–OHH-bonded to Six(OH)y, respectively [26,27]. It can be deduced that no extra framework of AlOH group ($AlOH_{efs}$) existed due to the unavailability of 3660–3690 cm^{-1}. This is expected since the catalysts were prepared by the impregnation method. As a consequence, metals were only introduced on the external surface of the zeolitic framework.

According to Kotrel et al. [28], OH species associated with IR band at 3608–3610 cm^{-1}, as being observed for all catalysts, is ascribed to the existence of catalytic activity that originates from the acid sites. The catalytic activity center is proven to have a number of Brønsted and Lewis acid sites. The Brønsted acid sites may originate from the Al (Al–OH) framework. On the other hand, the existence of Lewis acid sites can be due to the three-coordinated framework of aluminum formed upon dehydroxylation, non-framework alumina formed during dealumination, and charge balancing cations. The Brønsted acid strength has been thus linked to the Sanderson electronegativity and charge density of the framework [29], which suggests a long-range interaction and collective phenomenon for Brønsted acid strength. The strong IR band within this region strongly indicates that all the catalyst possess substantial amount of acid sites which is crucial for the catalytic activity to take place.

3.3. Surface area and pore size analysis

The results of BET analysis for all catalysts are presented in Table 1 alongside with TPR and TPD. It can be observed that HZSM-5 has the highest pore volume and among lowest pore diameter compared to the others. Fig. 5 illustrates the surface area and micropore versus percentage of olefin yield. The surface area and pore diameter of HZSM-5 is almost similar to that reported by Hoang [13]. HZSM-5 sample has the highest surface area followed by Al/ZSM-5. The lowest surface areas are given by Cr/ZSM-5 and Li/ZSM-5. The introduction of copper narrowed the pore diameter unlike other metals which increased the average pore diameter. However, the actual difference between HZSM-5 and Cu/ZSM-5 is very modest and within experimental error. It can be possible that loading copper on HZSM-5 did not change the average pore diameter. The increase in pore diameter for other catalysts other than copper might be due to the metals blocking the micropores and

Table 1
BET, TPR and TPD characterization results.

Catalysts	Pore volume (cm^3/g) ±5%[a]	Average pore diameter (A)	Amount of H_2 consumed (μmol/g)[b]	Desorbed amount, (μmol/g)[c]	Distribution of acid sites		
					Weak	Moderate	Strong
HZSM-5	0.238	23.696	30.96	1161.3	690.1	361.1	110.1
Al/ZSM-5	0.220	25.165	31.44	1116.4	715.8	255.2	145.4
Ca/ZSM-5	0.135	25.185	106.29	917.1	70.7	779.0	67.4
Cr/ZSM-5	0.213	29.086	62.86	1283.6	1032.7	250.9	0.0
Cu/ZSM-5	0.154	23.645	1100.28	1291.7	399.4	537.8	354.5
Li/ZSM-5	0.073	25.964	605.45	768.3	572.6	74.9	120.8
Mg/ZSM-5	0.157	26.346	36.63	1147.6	909.3	202.1	36.2
Ni/ZSM-5	0.173	25.528	1028.42	1236.2	820.3	372.3	43.6

[a] BET nitrogen adsorption method.
[b] Obtained from TPR.
[c] Obtained from TPD-NH_3.

as a consequence the average pore diameter was higher while there were still more macro and mesopores available as zeolites have macro, meso and micropores. In general, metal loading reduced the surface area, micropore area and pore volume of the parent HZSM-5 zeolite, but increased the average pore diameter of the metal-loaded HZSM-5.

3.4. TPD-NH_3 analysis

TPD was carried out to evaluate the acidic properties of the catalysts towards the formation of light olefin. Ammonia was adsorbed on acid sites of the catalysts due to its basic molecule nature. The point of the maximum temperature in the acidity versus temperature plot is a clue of NH_3 desorption activation energy magnitude and thus the relative acid strength of the sites [30]. Apart from the temperature maximum of the NH_3 desorption curve, the area under the desorption peak is also indicative of the relative number of acid sites present [30,31]. From the literature it is seen that there are three ranges of ammonia desorption: weak, intermediate and strong [32]. If desorption peak area is large then the number of acid sites is high.

Fig. 3 illustrates TPD-NH_3 profiles obtained from the catalysts. Several desorption peaks existed in all catalysts. Normally, strength of solid acid sites within TPD profiles can be classified by the temperature of desorption of NH_3 as weak (120–300 °C), moderate (300–500 °C) and strong (500–650 °C) [33]. From Fig. 3, it can be observed that all the curves displayed a major desorption peak around 150 °C, an indication of the weak (Brønsted and/or Lewis) sites present in the catalysts, which is consistent with typical ZSM-5 peak [31]. This range of peak corresponds to weak acid sites from surface hydroxyl groups [30] which is consistent with FTIR result discussed previously. The concentration of these sites was deemed to be not catalytically important [34], but it is assumed to effectively influence the proton mobility in zeolites [35]. A second much smaller desorption peak was obtained for HZSM-5 in the range of 350–450 °C, indicating the presence of strong Brønsted acid sites [31,34]. This peak is closely related to surface acid properties [11]. Cu/ZSM-5 has almost similar peak in the range of 350–460 °C but unlike HZSM-5, this peak is higher than the low temperature peak. The amount of acid sites for Ca/ZSM-5 in this region is the highest followed closely by Cu/ZSM-5. The peak in this range is supposed to be Brønsted acid sites formed by aluminum atoms connected to silicon by a so-called "bridging hydroxyl" where the negative charge generated is compensated for by a proton. This site is believed to be the main catalytic center and is also usually the most dominant one. As an acid site, it binds basic molecules such as ammonia via hydrogen bonds [36]. Cr/ZSM-5 which shows the second highest olefin selectivity and yield has low peaks in this region. This could indicate that in addition to acidic sites, the metal sites are active in the glycerol decomposition reactions.

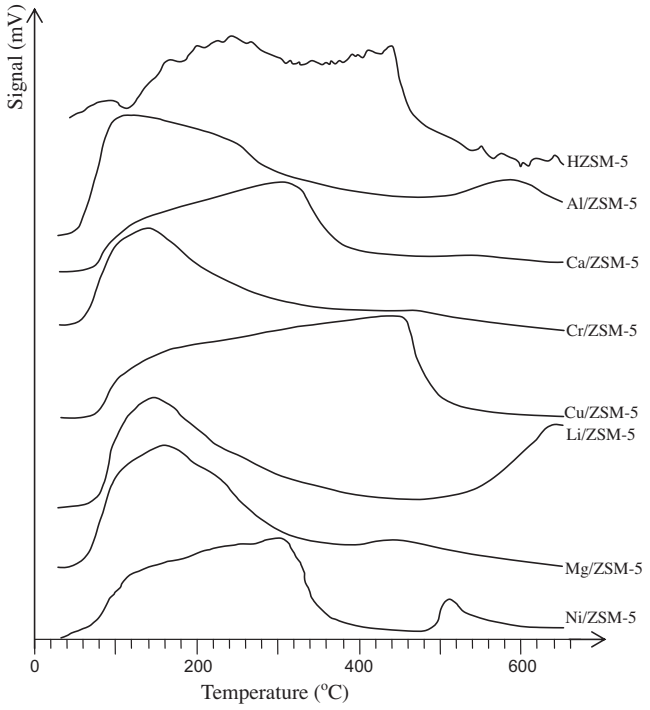

Fig. 3. Temperature program desorption ammonia (TPD-NH_3) profiles for HZSM-5 and modified ZSM-5 catalysts.

Lewis acid sites are composed of aluminum with low coordination or BBSi + ions formed from dehydroxylation in the thermal treatment at $T > 773$ K. These sites are also of importance in many catalytic processes such as Friedel–Crafts reactions, acting as an electron pair acceptor and thereby giving rise to charge transfer processes [37]. From the TPD-ammonia test, it can be inferred that the impregnation of metal induces new weak, moderate and strong acid sites differently. The deconvolution of TPD profiles of the catalysts into weak, moderate and strong Brønsted and Lewis acid sites was difficult, since the profiles overlaps. Therefore, the surface acidity was calculated as total acidity and expressed per μmol of NH_3 desorbed per gram of catalyst, between 100 and 650 °C [33]. The various acidic properties of catalysts is caused by the availability of crystallographically with different sittings and framework atoms dwelling in diverse environments [38].

3.5. TPR analysis

The amount of H_2 consumed can be referred from Table 1. Among the tested catalysts, Cu/ZSM-5 consumed most H_2. This is

followed closely by Ni/ZSM-5. The H_2 consumption by Ca/ZSM-5, Cr/ZSM-5, Al/ZSM-5, Mg/ZSM-5 and HZSM-5 were the lowest between 106.29 and 30.96 μmol/g. Fig. 4 illustrates the TPR results obtained from the catalysts. Generally it can be observed that all the catalyst have different reduction peak points. The reduction of bulk HZSM-5 results in four vague peaks at 80 °C, 350 °C, 420 °C and 520 °C. Despite peak existence, the reduction is deemed to be insignificant due to relatively low H_2 consumed for its reduction. Al/ZSM-5 has peaks at 180 °C and 315 °C. The lower temperature peaks possibly relate to low metal-support interaction caused by metal agglomeration of the aluminum on the zeolite surface. Ca/ZSM-5 has a peak at 550 °C and a minor shoulder peak at 650 °C. This is believed to be attributed to the Ca^{2+} reduced to Ca^{+} and further Ca^{0}. Cr/ZSM-5 has one low peak at 80 °C and a high peak at 395 °C. The peak at 395 °C is consistent with the TPR result of Cr/ZSM-5 spectrum reported by Mimura et al. [39] and possibly corresponds to the chromium occupying aluminum positions on the surface of ZSM-5 catalyst. This peak is the point where Cr^{3+} is reduced to Cr^{0}. Beyond the temperature, no additional peak was observed. Cu/ZSM-5 has a reduction point with peak at 290 °C and a small shoulder peak at 375 °C. The former peak is due to reduction of Cu^{2+} as detected from FTIR analysis to Cu^{+} and further reduced completely to Cu^{o} at 375 °C. The broad peaks may correspond to reduction of large copper particles that entered the catalyst pores decreasing the catalyst pore volume and diameter. As a consequence, higher amount of H_2 was required during adsorption to reduce the Cu^{2+} trapped within the pores. Li/ZSM-5 has an upward trend with huge reduction suggesting it requires substantial H_2 compared to the other catalyst due to strong metal-support interaction with ZSM-5 and the reduction of Li^{+} to Li^{0}. Mg/ZSM-5, like HZSM-5 has several vague peaks that adsorb less hydrogen for it to be reduced from Mg^{2+} to Mg^{0}. Ni/ZSM-5 has peaks at 370 °C, 405 °C and 560 °C. The Ni/ZSM-5TPR spectrum are generally similar to the patterns reported by Halliche [40]. The first peak corresponds to NiO-like species formed at the outer surface of the sample. Subsequently, the next peak is attributed to nickel ions that are secluded within the charge compensation sites of ZSM-5. The peak around 560 °C is a result of nickel oxide particles inside the zeolite channels that is more difficult to reduce [41]. Following this point all nickel ion has been reduced to Ni^{o}. The peak at 80 °C as displayed by Al/ZSM-5, Cr/ZSM-5 and Mg/ZSM-5 probably represents the reduction of small metal particles dispersed on catalysts.

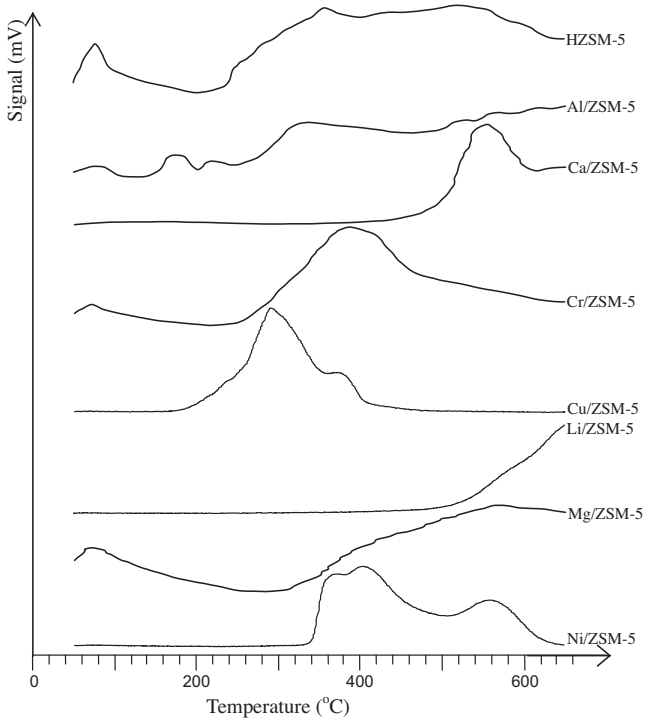

Fig. 4. Temperature program reduction profiles for HZSM-5 and modified ZSM-5 catalysts.

3.6. Catalyst activity

The catalytic activity in terms of gaseous product selectivity and yield is tabulated in Table 2 with complete glycerol conversion. Light olefins, paraffins, CO, CO_2 and hydrogen have been detected over all catalysts. The largest producer of ethylene in terms of gaseous selectivity is Cu/ZSM-5 (18.62%) followed by Cr/ZSM-5 (15.20%), HZSM-5, Al/ZSM-5 and Mg/ZSM-5. Ni/ZSM-5 and Ca/ZSM-5 both produced the lowest ethylene selectivity which is less than 3.5%. For propylene, the highest producer is Cr/ZSM-5 (2.60%) followed by Li/ZSM-5 (1.76%) Cu/ZSM-5, Ca/ZSM-5 and Ni/ZSM-5. Mg/ZSM-5 and Al/ZSM-5 both produced the lowest selectivity of propylene. It can be observed that for all catalysts the relative percentage produced for ethylene is the most, followed by far less propylene. Nonetheless, butylene was observed over Cr/ZSM-5, Li/ZSM-5 and Cu/ZSM-5 catalysts only.

For individual gaseous selectivity, HZSM-5 produced the largest amount of CO while Cr/ZSM-5 produced the largest CO_2 compared to other catalysts. Both CO and CO_2 were undesired products in the reaction produced due to the cracking reaction of light olefins (ethylene). Coking directly poisoned the catalyst and diminished catalytic activity. From the experimental observation, the amounts of CO and CO_2 at the starting of reaction were small. However, towards the end, CO and CO_2 and coke began to form due to the cracking of ethylene. Coking inhibited the production of light olefins and paraffin due to poisoning of the catalytic active sites. Al/ZSM-5 and Cr/ZSM-5 produced the highest amounts of CO and CO_2, respectively.

Methane was detected in all runs with reasonable percentage of gaseous selectivity (4.74–9.63%). This indicates that all catalysts are capable in breaking up glycerol into the smallest fraction of hydrocarbon. The existence of C_2, C_3 and C_4 olefins and paraffins originates from multiple complex reactions within the glycerol reaction network [8]. However, it is believed that the C_2–C_4 olefin and paraffin formation did not result from the oligomerization of methyl radicals. Instead, they were mainly formed from various consecutive dehydration, dehydrogenation and deoxidation processes of glycerol molecule itself [11].

Traces of hydrogen were observed over majority of the catalysts. It was found that only HZSM-5 and Cu/ZSM-5 did not produce hydrogen. The hydrogen produced from HZSM-5 and Cu/ZSM-5 could have been involved in several hydrogenation reactions. During the process, dehydrogenation released hydrogen which most likely be attracted by unstable species such as protonated 3-hydroxypropanal and protonated hydroxyacetone to produce more stable product. Ni/ZSM-5 on the other hand produced the highest hydrogen compared to other catalysts. The high selectivity in hydrogen is expected because of nickel's role as a hydrogen producer (reforming catalyst) [42].

Based in Fig. 5, no clear correlation between the physico-chemical properties and yield of light olefins can be confirmed. The surface and micropore areas of Al/ZSM-5 and Ni/ZSM-5 were the largest, but yields and selectivities of light olefins did not follow suit. As for Li/ZSM-5 which has the lowest surface and micropore area, it did not produce the highest light olefins selectivity either. Hence, in general, it can be deduced that the physical properties

Table 2
Gaseous selectivity and yield of products.

	HZSM-5		Al/ZSM-5		Ca/ZSM-5		Cr/ZSM-5		Cu/ZSM-5		Li/ZSM-5		Mg/ZSM-5		Ni/ZSM-5	
	Gaseous selectivity (%)	Product yield (%)	Gaseous selectivity (%)	Product yield (%)	Gaseous selectivity (%)	Product yield (%)	Gaseous selectivity (%)	Product yield (%)	Gaseous selectivity (%)	Product yield (%)	Gaseous selectivity (%)	Product yield (%)	Gaseous selectivity (%)	Product yield (%)	Gaseous selectivity (%)	Product yield (%)
CH_4	4.74	2.38	9.63	7.85	5.95	2.90	8.16	7.96	5.60	4.50	6.04	2.10	5.457	3.72	7.21	7.05
C_2H_6	0.18	0.09	0.61	0.50	0.34	0.16	0.73	0.72	0.43	0.35	0.23	0.08	0.516	0.35	0.20	0.20
C_2H_4	7.94	3.99	6.45	5.26	3.95	1.93	15.20	14.82	18.62	14.97	2.61	0.90	6.142	4.19	3.27	3.20
C_3H_8	0.11	0.05	0.05	0.04	0.00	0.00	0.57	0.56	0.07	0.06	0.40	0.14	0.062	0.04	0.14	0.14
C_3H_6	0.35	0.18	0.07	0.06	0.83	0.41	2.60	2.53	1.06	0.86	1.76	0.61	0.271	0.19	0.56	0.55
C_4H_{10}	0.00	0.00	0.00	0.00	0.00	0.00	0.20	0.19	0.00	0.00	0.26	0.09	0.000	0.00	0.00	0.00
C_4H_8	0.00	0.00	0.00	0.00	0.00	0.00	0.96	0.93	0.56	0.45	0.96	0.33	0.000	0.00	0.00	0.00
C_5H_{10}	0.00	0.00	0.00	0.00	1.16	0.57	1.39	1.35	0.00	0.00	0.49	0.17	0.329	0.22	0.00	0.00
CO	80.91	40.62	63.59	51.85	66.06	32.26	42.27	41.22	50.06	40.24	49.57	17.20	63.576	43.37	36.58	35.77
CO_2	5.76	2.89	15.16	12.36	15.78	7.70	24.19	23.59	23.60	18.97	11.90	4.13	16.444	11.22	21.18	20.71
H_2	0.00	0.00	4.44	3.62	5.93	2.90	3.74	3.64	0.00	0.00	25.77	8.94	7.204	4.91	30.85	30.16
Liquid		49.73		18.43		51.12		2.42		19.54		65.25		31.73		2.21
Coke		0.07		0.04		0.05		0.05		0.07		0.06		0.06		0.03

from metal-loading is not the prime reason that triggered the formation of light olefins.

Fig. 6 illustrates the relationship between light olefin yield and acidity of the catalysts. It can be observed that Cu/ZSM-5 with the highest total acid sites displayed the highest light olefins yield followed closely by Cr/ZSM-5. The introduction of copper as an effective catalyst support for the dehydration of glycerol [43] increases catalyst activity but at the same time favors sintering which lead to relatively low surface area. Insertion of chromium operates as a stabilizer to minimize sintering on the catalyst surface. This ensured Cr/ZSM-5, despite being a good dehydration catalyst to be in high activity state [44]. On the other hand Ca/ZSM-5 and Li/ZSM-5 catalysts that showed lower amount of acid sites correspond by producing lower light olefin selectivity. However, the trend was different for Ni/ZSM-5 which has relatively higher acid sites but produced the lowest light olefin selectivity. This is mainly because Ni/ZSM-5 produced the most CH_4 and H_2 gaseous selectivity and one of the highest CH_4 product yield. This is expected due to the fact that Ni/ZSM-5 has the tendency to be more active which results in excess degradation of glycerol to form lower-molecular gases [44]. This maybe also because nickel addition creates strong adsorption of glycerol molecules that would result in high potential for C–C bonds to be broken, thus explaining more CH_4 being produced compared to the other catalysts. The total acid sites may originate from the physical changes on the catalyst surface (as a result of metal loading) and resulted to formation of new several weak, moderate and strong acid sites. In general, the acid sites in the catalysts are responsible for the dehydration of glycerol [8,10]. Being a strong reductant at high temperature, glycerol can easily be reduced when metal centers with high valences are available [45].

In all experiments, olefin and paraffin were produced immediately after the introduction of glycerol vapor in the reactor. This means that the reaction takes place as soon as the reactant entered the reactor. In most of the reactions, olefins were the superior products from the beginning but decreases towards the 20 min mark. The olefin production supersedes that of paraffin possibly due to the cracking of paraffin taking place. In this most probably protolysis of feed molecule by Bronsted acid proton site was initiated. The protolysis reactions are one type of disproportionation that resulted in paraffin reduction to olefins [46]. However for Ni/ZSM-5, the paraffin was the more dominant product. Nickel on its own is a good hydrogenation catalyst. At lower temperatures (100–300 °C), it hydrogenates olefins to paraffins and at higher temperatures (>500 °C) it reforms alkenes and alkanes to hydrogen. As a consequence for Ni/ZSM-5, the formed olefins are hydrogenated to paraffins since the olefin amount is low. Specifically, methane was the most prominent paraffin product from the reaction of Ni/ZSM-5. In all cases, it can be observed that the CO and CO_2 productions tend to increase with time. At the 20 min point, the CO production rate is the highest. Although CO_2 production is not as high as CO, the trend is still the same as that of CO.

Ethylene was the major product followed by propylene while traces of butylene can only be noticed in some of the catalysts. At $t = 1$, ethylene has been largely produced for all catalyst and then it gradually decreased. The decrease of ethylene was expected as the catalyst became unactive due to coke poisoning. The formation of carbonaceous deposits or coke is an undesired product that appeared from side reactions taking place for almost all reactions of hydrocarbons and alcohols over acidic catalysts. Besides that, reaction temperature and the type of reactant feed will significantly influence coking during catalysis on any acidic catalyst [33]. This effect was observed to be more obvious for Cu/ZSM-5 which is due to higher amount of acid sites and its narrow pores. However, Cu/ZSM-5 managed to produce the highest light olefins before it deactivated. From this finding, it can be deduced that

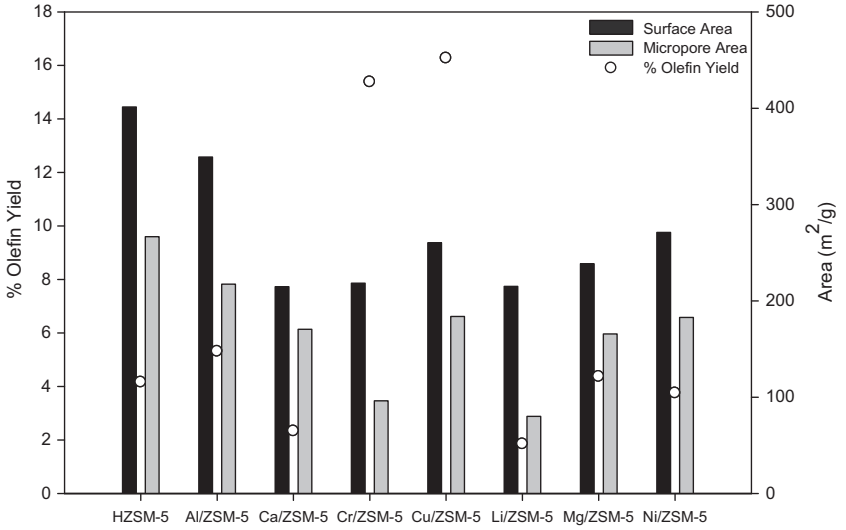

Fig. 5. Olefin yield distribution with surface and miropore areas of catalyst.

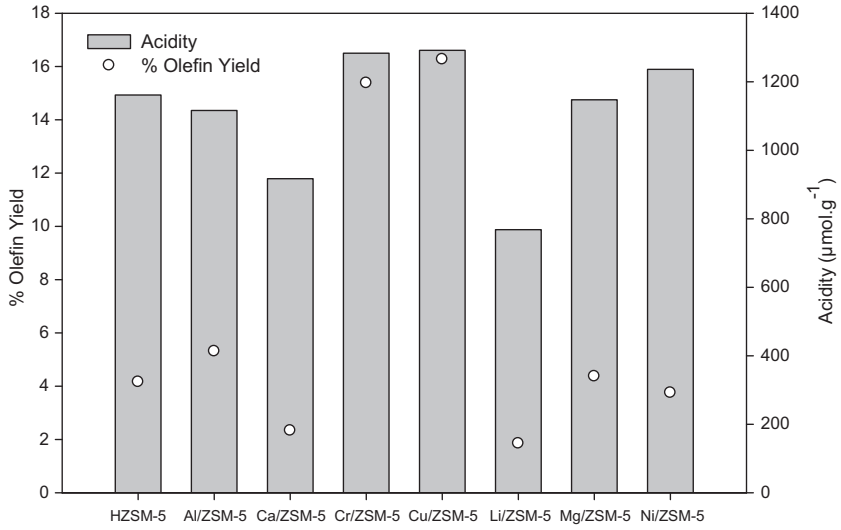

Fig. 6. Olefin yield distribution with catalyst acidity.

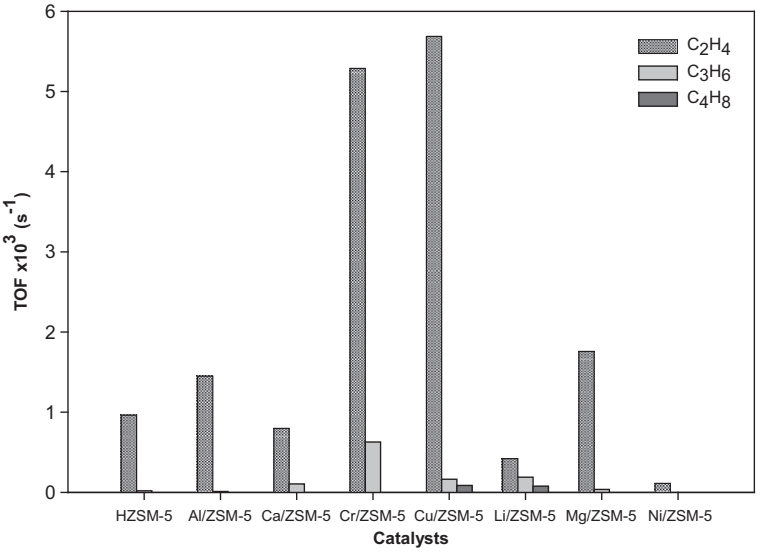

Fig. 7. TOF of olefins for various catalysts.

Cu/ZSM-5 with the smallest pore size is more selective towards ethylene and propylene (before catalyst deactivation). Thus, the activity in the glycerol dehydration and selectivity towards light olefin seem to depend on acid strength and pore size.

Fig. 7 illustrates the TOF of respective components of olefin, namely ethylene, propylene and butylene taken between 5 and 15 min. The TOF here is defined as equal to the rate of olefin molecule produced per second per surface area of the catalyst. As observed, the TOF of ethylene for Cu/ZSM-5 and Cr/ZSM-5 were significantly greater than the TOF of other species. This strongly indicates that the high olefin yield produced by Cu/ZSM-5 and Cr/ZSM-5 were largely contributed by ethylene formation. The TOF for propylene for all catalysts were below 1 s^{-1} while for butylene, it is almost negligible. Cu/ZSM-5 produced more olefin compared to other catalysts in its available acid sites. It is noted that the catalyst surface area containing active acid sites for Cr/ZSM-5 is lower than Cu/ZSM-5, but the amount of acid sites in the latter is superior, as confirmed by the TPD analysis. Earlier TPR data showed relatively huge magnitude of copper ions (to be reduced) are available on the catalyst surface. The copper ions are incorporated at two locations which are on the surface and inside the pores. This fact is consistent with the report by Moretti [47] that most active sites in Cu/ZSM-5 comprised of two close copper ion groups. This copper ions is believed to be responsible in actively producing the C_2–C_4 olefins. The reduced Cu^{2+} alongside with the strong and moderate acid sites played a key role for glycerol to undergo proton catalyzed dehydration which then lead to the trigger of several reactions such as dehydration, dehydrogenation, hydrogenation, dissociation and coupling. The reduction of Cu^{2+} may influenced the acid sites to lower the activation barriers for the dehydration of protonated glycerol [48], thus leading to the formation of light olefins. This is strengthened by TPR results which revealed that the most active catalysts, Cu/ZSM-5 and Cr/ZSM-5 were reduced at relatively lower temperatures compared to other metals.

There may be other reasons beside the surface area that account for higher TOF of Cu/ZSM-5 and Cr/ZSM-5. It seems that dispersion of copper and chromium on ZSM-5 has into certain extent created suitable environment for the breaking down of glycerol into smaller compounds. The amount of macro, meso and micropores might be different since the average pore diameter is different. This affects the type of acidic sites available on the catalyst surface. The influence of copper and chromium to the catalyst has resulted in substantial acid strength and acid sites ample to produce the most light olefins relative to others, as shown in the TPD findings. Al/ZSM-5 and Ni/ZSM-5 has acidity slightly lower than Cr/ZSM-5 but significantly lower olefin yield. For this, the role of nickel as hydrogen producer is well known [14,42], hence the low production of light olefin is expected because it hydrogenates olefin at the investigated temperatures. Al/ZSM-5 on the other hand produce low light olefin because it does not have combination of optimum physical and chemical properties. Li/ZSM-5 and Ca/ZSM-5 showed low total olefin TOF, 0.69 s^{-1} and 0.9 s^{-1}, respectively, due to the lack of acid sites in the catalyst. This is supported from TPD result where both catalysts displayed the lowest ammonia desorbtion compared to others. From TPR result, peak for Li/ZSM-5 is projected to be higher than other catalysts. At 650 °C, Li/ZSM-5 has not reached the reduction peak yet although it is in inclining trend. This shows that the reduction temperature is too high for important reactions involving olefin formation to take place since the operating temperature of the catalytic testing is 600 °C. The high absorption of hydrogen from TPR at such temperature inferred that any catalytic activity for Li/ZSM-5 will be optimal at temperature more than 650 °C. This may be the main reason why Li/ZSM-5 produced the lowest olefin in this study.

In general, there is no clear correlation between surface area and the metal content. Other reasons such as the influence of supporting material and human error in preparation methods could have accounted for the differences in the surface areas [49]. In addition, different pore sizes and acidic sites should also be taken into account.

There are many reaction schemes proposed for the dehydration of glycerol [5,8,11,45,48,50]. However, none of the reaction schemes proposed is dedicated specifically on the formation of light olefin. A plausible reaction scheme for glycerol conversion to light olefins is shown in Fig. 8. Acidic catalyst used in this study resulted in glycerol to undergo dehydration process to form 3-hydroxypropanal. In actual, the dehydration of glycerol can also precede via the formation of acetol [8,48,51]. However, 3-hydroxypropanal is a more feasible option because of its tendency to break up further to acetaldehyde and formaldehyde; and vinyl alcohol and formaldehyde. Vinyl alcohol under the catalytic reaction

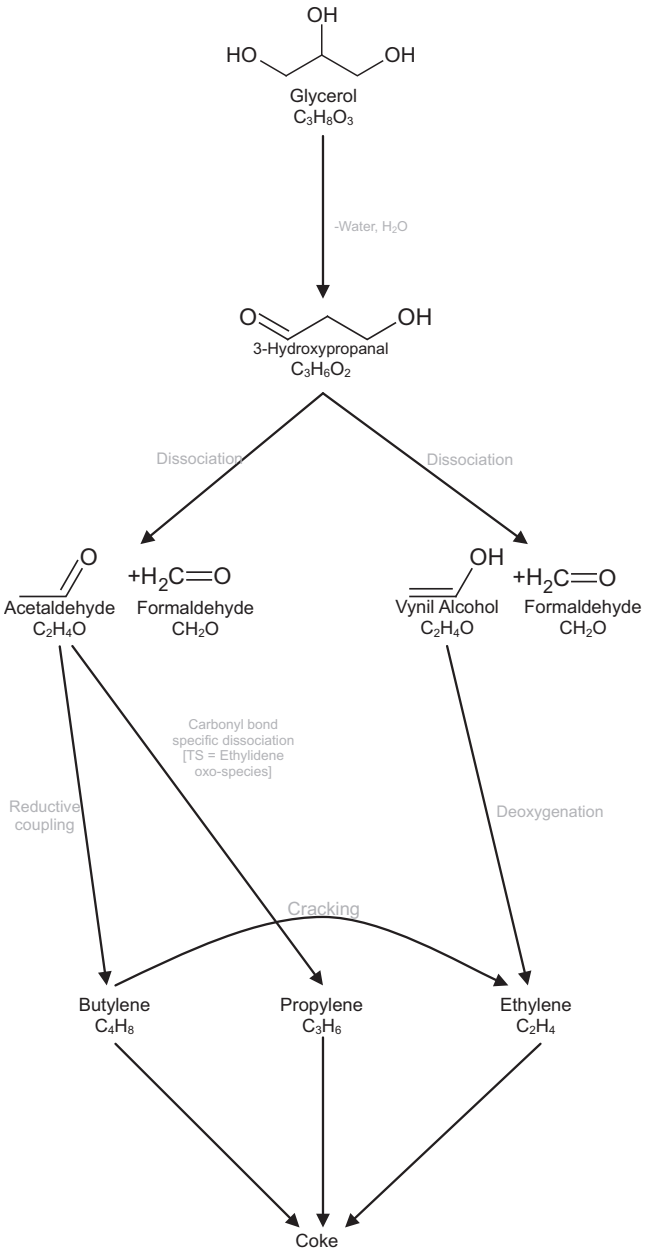

Fig. 8. Proposed reaction scheme for glycerol conversion to light olefins.

condition will undergo deoxygenation process, releasing oxygen to form ethylene. At the same time, other side reactions involving acetaldehyde will trigger the formation of propylene and butylene. Acetaldehyde will undergo carbonyl bond specific dissociation [TS = Ethylidene oxo-species] to form propylene. At the same time protonated acetaldehyde will couple within itself to undergo reductive coupling to form butylene. From the experiment, the production of butylene was almost negligible and this can be explained by the cracking of butylene to form ethylene. Despite the formation of ethylene, propylene and butylene, continuous heating experienced by olefin remaining in the hydrocarbon pool of zeolite network will result to gradual C–H bond eventually broken, via dehydrogenation process, thus resulted to coke formation on catalyst surface. This is consistent with the mechanistic model where coke is formed in pyrolysis units producing ethylene [52]. Furthermore, coke precursors prefer to form on surface with moderate to strong acid sites, which then finally lead to catalyst deactivation. Further work is under progress to study the reaction scheme in more detail.

4. Conclusion

Catalyst screening of various metal-impregnated HZSM-5 for catalytic conversion of glycerol to olefins has been carried out by testing its performance in a quartz tube fixed-bed reactor. The loading of metals into HZSM-5 zeolite enhanced the acid sites needed for the glycerol dehydration. Metal-loading was responsible for the physical changes that can be observed from the surface area, micropore area and pore volume. However, no direct relationship can be deduced from the physical properties. Metal impregnation of the parent HZSM-5 catalyst has resulted in the diversity of low, medium and strong acid sites of the catalysts. Cu/ZSM-5, displayed more moderate to strong acid sites compared to others, produced the highest TOF with 16.3% light olefin yield.

Acknowledgements

The authors would like to acknowledge Ministry of Higher Education, Malaysia (MOHE) for the financial supports received for this work through the project number (Vot 78401) under Fundamental Research Grant Scheme (FRGS) and Universiti Teknologi Malaysia (UTM).

References

[1] M.J. Haas, Improving the economics of biodiesel production through the use of low value lipids as feedstocks: vegetable oil soapstock, Fuel Process. Technol. 86 (2005) 1087–1096.
[2] R.S. Karinen, A.O.I. Krause, New biocomponents from glycerol, Appl. Catal. A: Gen. 306 (2006) 128–133.
[3] T.L. Chew, S. Bhatia, Catalytic processes towards the production of biofuels in a palm oil and oil palm biomass-based biorefinery, Bioresour. Technol. 99 (2008) 7911–7922.
[4] G.W. Huber, A. Corma, Synergies between bio- and oil-refineries for the production of fuels from biomass, Angew. Chem. – Int. Ed. 46 (2007) 7184–7201.
[5] K. Pathak, K.M. Reddy, N.N. Bakhshi, A.K. Dalai, Catalytic conversion of glycerol to value added liquid products, Appl. Catal. A: Gen. 372 (2010) 224–238.
[6] A. Wolfson, C. Dlugy, Y. Shotland, Glycerol as a green solvent for high product yields and selectivities, Environ. Chem. Lett. 5 (2007) 67–71.
[7] H. Serafim, I.M. Fonseca, A.M. Ramos, J. Vital, J.E. Castanheiro, Valorization of glycerol into fuel additives over zeolites as catalysts, Chem. Eng. J. 178 (2011) 291–296.
[8] A. Corma, G.W. Huber, L. Sauvanaud, P. O'Connor, Biomass to chemicals: catalytic conversion of glycerol/water mixtures into acrolein, reaction network, J. Catal. 257 (2008) 163–171.
[9] A.S. de Oliveira, S.J.S. Vasconcelos, J.R. de Sousa, F.F. de Sousa, J.M. Filho, A.C. Oliveira, Catalytic conversion of glycerol to acrolein over modified molecular sieves: activity and deactivation studies, Chem. Eng. J. 168 (2011) 765–774.
[10] B. Katryniok, S. Paul, M. Capron, F. Dumeignil, Towards the sustainable production of acrolein by glycerol dehydration, ChemSusChem 2 (2009) 719–730.
[11] K. Murata, I. Takahara, M. Inaba, Propane formation by aqueous-phase reforming of glycerol over Pt/H-ZSM5 catalysts, React. Kinet. Catal. Lett. 93 (2008) 59–66.
[12] S.J.S. Vasconcelos, C.L. Lima, J.M. Filho, A.C. Oliveira, E.B. Barros, F.F. de Sousa, M.G.C. Rocha, P. Bargiela, A.C. Oliveira, Activity of nanocasted oxides for gas-phase dehydration of glycerol, Chem. Eng. J. 168 (2011) 656–664.
[13] T.Q. Hoang, X. Zhu, T. Danuthai, L.L. Lobban, D.E. Resasco, R.G. Mallinson, Conversion of glycerol to alkyl-aromatics over zeolites, Energy Fuels 24 (2010) 3804–3809.
[14] S. Adhikari, S.D. Fernando, A. Haryanto, Hydrogen production from glycerin by steam reforming over nickel catalysts, Renew. Energy 33 (2008) 1097–1100.
[15] C.-H. Zhou, J.N. Beltramini, Y.-X. Fan, G.Q. Lu, Chemoselective catalytic conversion of glycerol as a biorenewable source to valuable commodity chemicals, Chem. Soc. Rev. 37 (2008) 527–549.
[16] M. Pagliaro, M. Rossi, The Future of Glycerol New Usages of a Versatile Raw Material, RSC Green Chemistry Book Series, UK, 2008.
[17] F.C. Patcas, The methanol-to-olefins conversion over zeolite-coated ceramic foams, J. Catal. 231 (2005) 194–200.
[18] J.W. Park, S.J. Kim, M. Seo, S.Y. Kim, Y. Sugi, G. Seo, Product selectivity and catalytic deactivation of MOR zeolites with different acid site densities in methanol-to-olefin (MTO) reactions, Appl. Catal. A: Gen. 349 (2008) 76–85.
[19] I. Takahara, M. Saito, M. Inaba, K. Murata, Dehydration of ethanol into ethylene over solid acid catalysts, Catal. Lett. 105 (2005) 249–252.
[20] M. Inaba, K. Murata, M. Saito, I. Takahara, Ethanol conversion to aromatic hydrocarbons over several zeolite catalysts, React. Kinet Catal. Lett. 88 (2006) 135–141.
[21] X. Li, B. Shen, Q. Guo, J. Gao, Effects of large pore zeolite additions in the catalytic pyrolysis catalyst on the light olefins production, Catal. Today 125 (2007) 270–277.
[22] M. Masih, I. Algahtani, L. De Mello, Price dynamics of crude oil and the regional ethylene markets, Energy Econom. 32 (2010) 1435–1444.
[23] Z. Peiqing, W. Xiangsheng, G. Xinwen, G. Hongchen, Z. Leping, H. Yongkang, Characterization of modified nanoscale ZSM-5 zeolite and its application in the olefins reduction in FCC gasoline, Catal. Lett. 92 (2004) 63–68.
[24] H.A. Zaidi, K.K. Pant, Catalytic activity of copper oxide impregnated HZSM-5 in methanol conversion to liquid hydrocarbons, Can. J. Chem. Eng. 83 (2005) 970–977.
[25] Y.-J. Jiang, J.C. Juan, X.-J. Meng, W.-L. Cao, M.A. Yarmo, J.-C. Zhang, Preparation and Catalytic Application of Novel Water Tolerant Solid Acid Catalysts of Zirconium Sulfate/HZSM-5, vol. 23, Chemical Research in Chinese Universities, 2007 (349–354).
[26] F. Jin, Y. Li, A FTIR and TPD examination of the distributive properties of acid sites on ZSM-5 zeolite with pyridine as a probe molecule, Catal. Today 145 (2009) 101–107.
[27] I. Halasz, M. Agarwal, B. Marcus, W.E. Cormier, Molecular spectra and polarity sieving of aluminum deficient hydrophobic H-Y zeolites, Microporous Mesoporous Mater. 84 (2005) 318–331.
[28] S. Kotrel, M.P. Rosynek, J.H. Lunsford, Quantification of acid sites in H-ZSM-5, H-β, and H-Y zeolites, J. Catal. 182 (1999) 278–281.
[29] X. Liu, Infrared and Raman Spectroscopy Zeolite Characterization and Catalysis, in: A.W. Chester, E.G. Derouane (Eds.), Springer Netherlands, 2010, pp. 197–222.
[30] L. Rodríguez-González, F. Hermes, M. Bertmer, E. Rodríguez-Castellón, A. Jiménez-López, U. Simon, The acid properties of H-ZSM-5 as studied by NH_3-TPD and 27Al-MAS-NMR spectroscopy, Appl. Catal. A: Gen. 328 (2007) 174–182.
[31] R. López-Fonseca, J.I. Gutiérrez-Ortiz, M.A. Gutiérrez-Ortiz, J.R. González-Velasco, Catalytic combustion of chlorinated ethylenes over H-zeolites, J. Chem. Technol. Biotechnol. 78 (2003) 15–22.
[32] M. Lewandowski, Z. Sarbak, The effect of boron addition on hydrodesulfurization and hydrodenitrogenation activity of $NiMo/Al_2O_3$ catalysts, Fuel 79 (2000) 487–495.
[33] W. Suprun, M. Lutecki, T. Haber, H. Papp, Acidic catalysts for the dehydration of glycerol: activity and deactivation, J. Mol. Catal. A: Chem. 309 (2009) 71–78.
[34] M. Niwa, N. Katada, Measurements of acidic property of zeolites by temperature programmed desorption of ammonia, Catal. Surveys Jpn. 1 (1997) 215–226.
[35] M.E. Franke, U. Simon, Solvate-supported proton transport in zeolites, ChemPhysChem 5 (2004) 465–472.
[36] F. Lónyi, J. Valyon, On the interpretation of the NH_3-TPD patterns of H-ZSM-5 and H-mordenite, Microporous Mesoporous Mater. 47 (2001) 293–301.
[37] M.H.W. Sonnemans, C. Den Heijer, M. Crocker, Studies on the acidity of mordenite and ZSM 5. 2. Loss of broensted acidity by dehydroxylation and dealumination, J. Phys. Chem. 97 (1993) 440–445.
[38] L. Damjanović, A. Auroux, Determination of Acid/Base Properties by Temperature Programmed Desorption (TPD) and Adsorption Calorimetry Zeolite Characterization and Catalysis, in: A.W. Chester, E.G. Derouane (Eds.), Springer, Netherlands, 2010, pp. 107–167.
[39] N. Mimura, M. Okamoto, H. Yamashita, S.T. Oyama, K. Murata, Oxidative dehydrogenation of ethane over Cr/ZSM-5 catalysts using CO_2 as an oxidant, J. Phys. Chem. B 110 (2006) 21764–21770.
[40] D. Halliche, O. Cherifi, A. Auroux, Microcalorimetric studies and methane reforming by CO_2 on Ni-based zeolite catalysts, Thermochim. Acta 434 (2005) 125–131.
[41] T.E. Solh, K. Jarosch, H.I. de Lasa, Fluidizable catalyst for methane reforming, Appl. Catal. A: Gen. 210 (2001) 315–324.

[42] A. Iriondo, V. Barrio, J. Cambra, P. Arias, M. Güemez, R. Navarro, M. Sánchez-Sánchez, J. Fierro, Hydrogen production from glycerol over nickel catalysts supported on Al_2O_3 modified by Mg, Zr, Ce or La, Top. Catal. 49 (2008) 46–58.
[43] S. Sato, M. Akiyama, R. Takahashi, T. Hara, K. Inui, M. Yokota, Vapor-phase reaction of polyols over copper catalysts, Appl. Catal. A: Gen. 347 (2008) 186–191.
[44] C.-W. Chiu, M.A. Dasari, G.J. Suppes, W.R. Sutterlin, Dehydration of glycerol to acetol via catalytic reactive distillation, AIChE J. 52 (2006) 3543–3548.
[45] J. Deleplanque, J.L. Dubois, J.F. Devaux, W. Ueda, Production of acrolein and acrylic acid through dehydration and oxydehydration of glycerol with mixed oxide catalysts, Catal. Today 157 (2010) 351–358.
[46] C. Liu, X. Gao, Z. Zhang, H. Zhang, S. Sun, Y. Deng, Surface modification of zeolite Y and mechanism for reducing naphtha olefin formation in catalytic cracking reaction, Appl. Catal. A: Gen. 264 (2004) 225–228.
[47] G. Moretti, Turnover frequency for NO decomposition over Cu–ZSM-5 catalysts: insight into the reaction mechanism, Catal. Lett. 28 (1994) 143–152.
[48] M.R. Nimlos, S.J. Blanksby, X. Qian, M.E. Himmel, D.K. Johnson, Mechanisms of glycerol dehydration, J. Phys. Chem. A 110 (2006) 6145–6156.
[49] A. Bienholz, H. Hofmann, P. Claus, Selective hydrogenolysis of glycerol over copper catalysts both in liquid and vapour phase: correlation between the copper surface area and the catalyst's activity, Appl. Catal. A: Gen. 391 (2011) 153–157.
[50] W. Yan, G.J. Suppes, Low-pressure packed-bed gas-phase dehydration of glycerol to acrolein, Ind. Eng. Chem. Res. 48 (2009) 3279–3283.
[51] T. Laino, C. Tuma, A. Curioni, E. Jochnowitz, S. Stolz, A revisited picture of the mechanism of glycerol dehydration, J. Phys. Chem. A 115 (2011) 3592–3595.
[52] L.F. Albright, J.C. Marek, Mechanistic model for formation of coke in pyrolysis units producing ethylene, Ind. Eng. Chem. Res. 27 (1988) 755–759.